

Computational Acoustics based on Conservation Equations using Taylor Hood Finite Elements

M. Kaltenbacher¹ and A. Hüppe²

¹ *Applied Mechatronics, University of Klagenfurt, Austria, Email: manfred.kaltenbacher@uni-klu.ac.at*

² *Applied Mechatronics, University of Klagenfurt, Austria, Email: andreas.hueppe@uni-klu.ac.at*

Introduction

We concentrate on the efficient solution of enhanced wave problems, which are mathematically modeled by their conservation equations, namely the mass and momentum conservation. Such formulations arise, e.g., in computational aeroacoustics or acoustic propagation in flowing media. Even for acoustic wave propagations, where an acoustic wave equation exists, formulations based on the conservation equations have the advantage, that the numerical solution provides directly the two main engineering quantities, the acoustic pressure and the acoustic particle velocity.

Governing Equations

Our final goal is the numerical computation of flow induced sound based on a hybrid approach. Therewith, in a first step the flow is computed applying, e.g., a LES (Large Eddy Simulation) turbulence model, and in a second step the acoustic sound is calculated by the following set of partial differential equations (PDEs) [5, 4]

$$\frac{\partial \mathbf{v}'}{\partial t} + (\mathbf{U} \cdot \nabla) \mathbf{v}' + \frac{1}{\rho_0} \nabla p' = 0 \quad (1)$$

$$\frac{\partial p'}{\partial t} + \mathbf{U} \cdot \nabla p' + \rho_0 c^2 \nabla \cdot \mathbf{v}' = -\frac{DP}{Dt}. \quad (2)$$

In (1) and (2) p' denotes the acoustic pressure, \mathbf{v}' the acoustic particle velocity, \mathbf{U} the flow velocity, P the hydrodynamic pressure, ρ_0 the mean density of the fluid and c the speed of sound.

In the following, we set P and \mathbf{U} to zero, and will restrict to the pure acoustic problem setup. Therewith, we arrive at the momentum and mass equation for linear acoustics. By introducing appropriate test functions ψ and φ , multiplying the PDEs by these test functions and integrating over the computational domain Ω results in the corresponding weak formulation: Find $(\mathbf{v}', p') \in V \times Q$ such that

$$\int_{\Omega} \psi \cdot \frac{\partial \mathbf{v}'}{\partial t} \, d\Omega + \int_{\Omega} \frac{1}{\rho_0} \psi \cdot \nabla p' \, d\Omega = 0 \quad (3)$$

$$\int_{\Omega} \frac{\partial p'}{\partial t} \, d\Omega - \int_{\Omega} \rho_0 c^2 \mathbf{v}' \cdot \nabla \varphi \, d\Omega + \int_{\Gamma} \rho_0 c^2 \varphi \mathbf{v}' \cdot \mathbf{n} \, d\Gamma = 0 \quad (4)$$

for all $(\psi', \varphi) \in V \times Q$. Therein, V and Q are appropriate spaces and we have performed an integration by parts

concerning the divergence term of the acoustic particle velocity in (2). The so obtained boundary integral in (4) allows us to prescribe given mechanical vibration velocities \mathbf{v}_{mech} in normal direction along Γ (or parts of Γ , as it is the case for vibrational acoustics). Furthermore, the simple substitution

$$\mathbf{v}' \cdot \mathbf{n} = \frac{p'}{Z_0} = \frac{p'}{\rho_0 c} \quad (5)$$

with Z_0 the specific acoustic impedance allows us to approximate free radiation by a first order absorbing boundary condition.

Finite Element Formulation

The application of the standard Finite Element (FE) method to the acoustic conservation equations in its weak formulation expressed by (3) and (4) will result in an instable formulation [2]. In order to obtain stable finite elements, we need a mixed FE formulation and use $H(\text{div})$ functions for the approximation of the particle velocity and L_2 functions for the acoustic pressure [1]. However, it can be proofed, that approximating the acoustic particle velocity by Lagrangian finite elements one order higher than those for the acoustic pressure will also provide a stable formulation [2]. We will apply this approach and choose the following functional spaces

$$V_h \subset V = \mathcal{L}_q^1 \quad Q_h \subset Q = \mathcal{L}_{q-1}^1 \\ \mathcal{L}_q^1 = \{u \mid u|_K \in P_q(K), u \in H^1(\Omega)\}$$

with $P_q(K)$ the space of polynomials with degree $\leq q$ on the element K . Therewith, we arrive at the so-called Taylor-Hood elements, which will guarantee the correct discretization. For a proof we refer to [2].

Equipped with this framework, we approximate the physical quantities acoustic pressure and acoustic particle velocity by

$$p' \approx p'^h = \sum_{a=1}^{n_n} N_a^{q-1} p'_{ea} \quad (6)$$

$$\mathbf{v}' \approx \mathbf{v}'^h = \sum_{i=1}^{n_d} \sum_{a=1}^{n_n} N_a^q v'_{ia} \mathbf{e}_i. \quad (7)$$

Therein, n_n denotes the number of FE nodes, n_d the space dimension, q the order of the FE basis functions and \mathbf{e}_i the unit vector in i -direction.

Using the same ansatz for the test functions and substituting these approximations into the weak formulation

given by (3) and (4), we arrive at the following semi-discrete Galerkin formulation

$$\mathbf{M}^{vv} \underline{\dot{v}}' + \mathbf{K}^{vp} \underline{p}' = 0 ; \quad \underline{\dot{v}}' = \partial \underline{v}' / \partial t \quad (8)$$

$$\mathbf{M}^{pp} \underline{\dot{p}}' - \mathbf{K}^{pv} \underline{v}' = 0 ; \quad \underline{\dot{p}}' = \partial \underline{p}' / \partial t \quad (9)$$

$$(10)$$

with \underline{p}' and \underline{v}' the nodal vector of unknown acoustic pressure and acoustic particle velocity, respectively. The global FE matrices are obtained by the assembly procedure of the element matrices, which compute as follows:

$$\mathbf{m}_e^{vv} = [\mathbf{m}_{ab}] ; \quad \mathbf{m}_{ab} = \int_{\Omega^e} \mathbf{e}_i^t N_a^q N_b^q \mathbf{e}_j \, d\Omega \quad (11)$$

$$\mathbf{m}_e^{pp} = [m_{ab}] ; \quad m_{ab} = \int_{\Omega^e} N_a^{q-1} N_b^{q-1} \, d\Omega \quad (12)$$

$$\mathbf{k}_e^{vp} = [\mathbf{k}_{ab}] ; \quad \mathbf{k}_{ab} = \int_{\Omega^e} \frac{1}{\rho_0} N_a^q \mathbf{e}_i^t \nabla N_b^{q-1} \, d\Omega \quad (13)$$

$$\mathbf{k}_e^{pv} = [\mathbf{k}_{ab}] ; \quad \mathbf{k}_{ab} = \int_{\Omega^e} \rho_0 c^2 N_a^q \mathbf{e}_i^t \nabla N_b^{q-1} \, d\Omega \\ + \int_{\Gamma^e} \rho_0 c^2 N_a^{q-1} N_b^q \mathbf{e}_i^t \mathbf{n} \, d\Gamma. \quad (14)$$

The time discretization is performed by the general trapezoidal scheme, which reads, e.g., for the acoustic pressure as follows

$$\underline{p}'_{n+1} = \underline{p}'_n + \Delta t \left((1 - \gamma_P) \underline{\dot{p}}'_n + \gamma_P \underline{\dot{p}}'_{n+1} \right) \quad (15)$$

In (15) n denotes the time step, Δt the time step size and Γ_P the time discretization parameter. For $\gamma_P \in [0.5, 1]$ the scheme is fully implicit and A-stable [3].

Numerical Tests

For the following numerical tests we will compare our results with data obtained by solving the wave equation in pressure formulation using standard finite elements.

In a first example, we investigate the discretization error as a function of the number of finite elements per wavelength. Therewith, we perform a harmonic simulation of an acoustic wave within a channel as displayed in Figure 1. The wave number k is chosen to be $9\pi/2$ and we compute the resulting acoustic pressure on grids with reducing mesh size h . Within our Taylor-Hood approach we use first order elements for the acoustic pressure and second order elements for the acoustic particle velocity. The discretization error is obtained by comparing the numerical solution with the analytical one in each finite element, and we define the overall accumulated error E_a by

$$E_a = \sqrt{\frac{\sum_{i=1}^{n_n} (\hat{p}^h - \hat{p})^2}{\sum_{i=1}^{n_n} \hat{p}^2}}$$

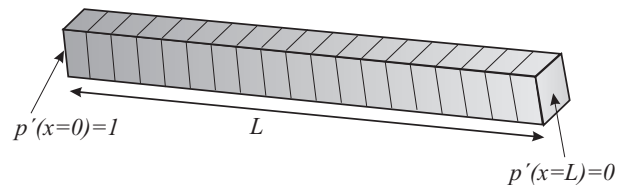


Figure 1: Acoustic wave in a channel with given Dirichlet boundary conditions.

with n_n the number of finite element nodes. The analytic solution \hat{p} computes by

$$\hat{p} = \cos(kx) - \frac{\cos(kL)}{\sin(kL)} \sin(kx).$$

Figure 2 shows the accumulated error E_a as a function

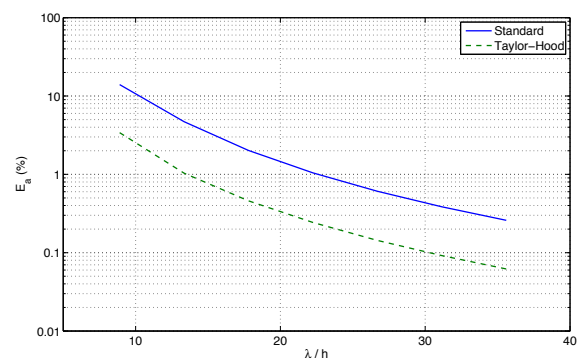


Figure 2: Reduction of accumulated error E_a as a function of the number of finite elements per wavelength.

of the finite elements per wavelength. The error behavior for both formulations, the Taylor-Hood approach solving the conservation equations (denoted by Taylor-Hood) and the standard finite elements solving the wave equation (denoted by Standard), is quite similar, except that the Taylor-Hood approach has a constant smaller error.

For the second investigation, we use the same setup, but keep the computational mesh fixed and change the wave number k (see Table 1) as well as the order q of the finite element basis functions. Figure 3 demonstrates that we

k	$9\pi/2$	$19\pi/2$	$29\pi/2$
λ/h	8.9	4.2	2.7

Table 1: Choice of wave number k and resulting number of finite elements per wavelength

obtain for both formulation an effective reduction of the overall accumulated error E_a by increasing the order q of the finite element basis functions. A closer look shows us, that the error reduction is stronger for the standard finite elements solving the wave equation as for the Taylor-Hood elements solving the conservation equations.

In a third example, we consider a sine pulse traveling through a channel and record the wave signal at a distance of three times the fundamental wavelength (see

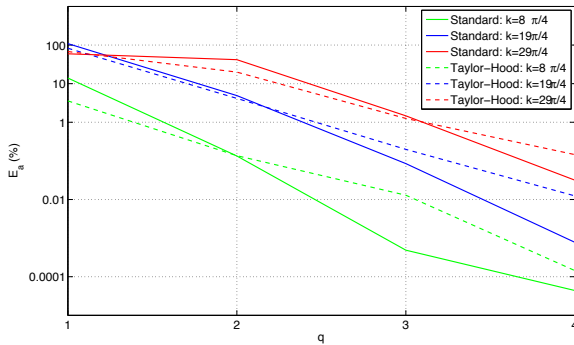


Figure 3: Reduction of accumulated error E_a as a function of the order q of the FE basis functions.

Figure 4). We prescribe the acoustic pressure on the left surface of the channel and apply first order absorbing boundary conditions to the right surface of the channel. Now, we have to perform space and time discretization, which are chose as a function of the main exciting frequency f_0 and main wavelength $\lambda_0 = c/f_0$.

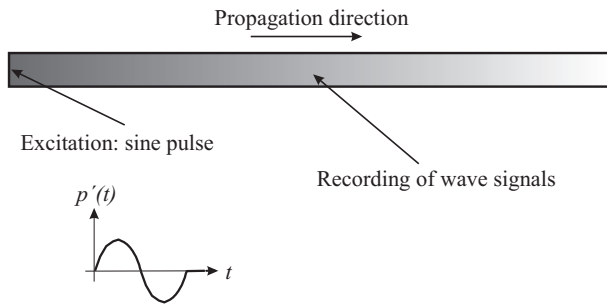


Figure 4: Setup of the transient case study.

In a first step, we just analyze our Taylor-Hood approach solving the conservation equations and investigate the influence of the choice of the time discretization parameter γ_P . We use a discretization in space of 20 finite elements per main wavelength λ_0 ($h = \lambda_0/20$) and a time step size Δt of $1/(30f_0)$. Now, it is well know, that the trapezoidal scheme has second order accuracy for $\gamma_P = 0.5$. For this choice the scheme is also called Crank-Nicolson scheme. Figure 5 displays three selected computations, which

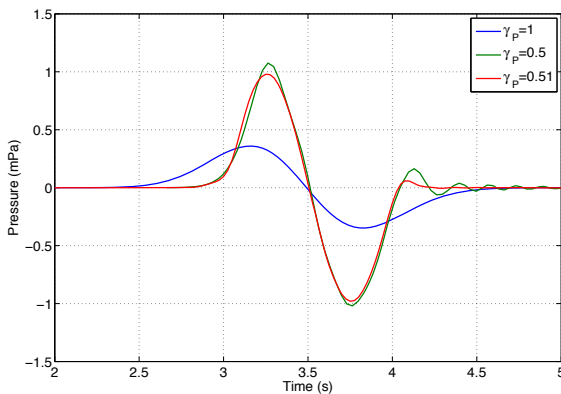


Figure 5: Acoustic pressure at a distance of 3λ computed by different time discretization parameter γ_P .

demonstrates two effects: First, the choice of $\gamma_P = 1$ leads to a strong damping of the wave, due to numerical dissipation, and therefore is useless for computing wave propagation over large distances. Second, choosing γ_P exactly 0.5 leads to some overshoot of the amplitude and numerical oscillations. Intensive numerical test showed, that with a value $\gamma_P = 0.51$ we achieve the best results, which is a compromise between reducing the oscillations and introducing not too much dissipation.

In a second step, we investigate in different space and time discretizations and compare the Taylor-Hood approach with the standard finite elements solving the acoustic wave equation, which has been discretized by the Newmark scheme using for the two parameters β_H and γ_H the values of 0.25 and 0.5 [3]. The results are displayed in

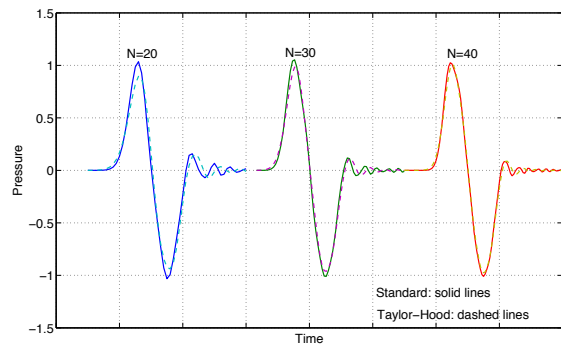


Figure 6: Acoustic pressure at a distance of 3λ computed for the three different discretizations: N denotes the number of finite elements as well as time steps with respect to the main wavelength λ_0 and main time period $T_0 = 1/f_0$.

Figure 6, where we have shifted the recorded pressures for display reasons. For all three combinations of space and time discretizations we obtain quite similar results. Just for the first case, where we used a space discretization of $h = \lambda_0/20$ and time discretization of $\Delta t = 1/(20f_0)$ the Taylor-Hood approach results in too small pressure amplitudes. Comparing these results with the results in Figure 5 we can conclude, that for our example of a pulse propagating in a channel the number of time steps per main time period T_0 should be larger than the number of finite elements per main wavelength λ_0 . This fact is confirmed by the results shown in Figure 7.

In a last example we now consider the wave propagation in a media with flow. Figure 8 displays the computational domain. We excite a wave by prescribing the normal velocity along a small part of the boundary. The time function of this excitation is a sine-pulse as used in the channel examples. This generated wave propagates within a flowing media, where the flow has a constant value 0.3 times the speed of sound and has the direction as indicated in Figure 8. Over the whole computational domain we generate a mesh with about 40 finite elements per main wavelength λ_0 and use a time step size of $\Delta t = 1/(50f_0)$. The generated pulse-wave strongly influenced by the flow is shown in Figure 9. One can clearly see the increased propagation speed and reduced

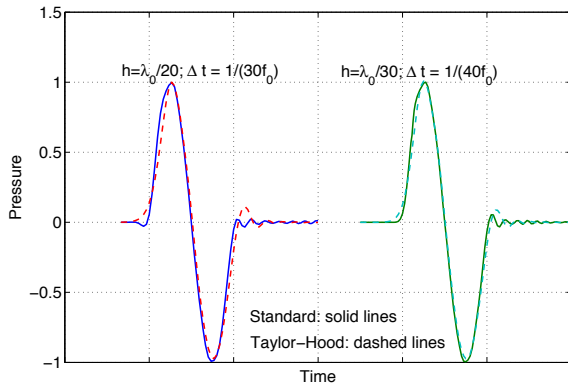


Figure 7: Acoustic pressure at a distance of 3λ computed by different space and time discretizations.

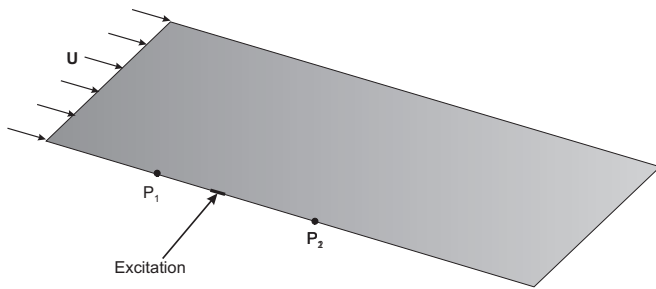


Figure 8: Computational setup for wave propagation in a flowing media.

pressure amplitude of the wave in downstream direction as well as the reduced propagation speed and increased amplitude in upstream direction. Furthermore, Figure 10 displays the acoustic pressure signals recorded at the two monitoring points P_1 (upstream) and P_2 (downstream).

Conclusion

We have demonstrated the applicability of Taylor-Hood elements for the stable discretization of the acoustic conservation equations. Therewith, we have shown their convergence behavior towards h-FEM (reducing the mesh size) and p-FEM (increasing the order of the FE basis functions). The results are quite comparable to the convergence behavior of standard finite elements solving the wave equation. In addition, we have shown

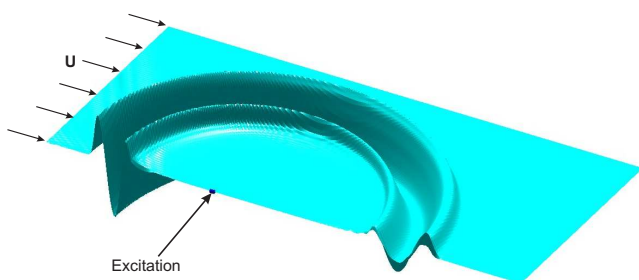


Figure 9: Acoustic pressure field in the flowing media at a characteristic time step.

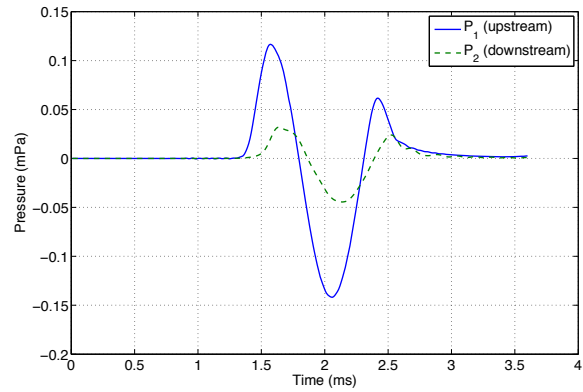


Figure 10: Acoustic pressure at the tow monitoring points. P_1 is at 1 m distance in upstream and P_2 at 2 m distance in downstream direction from the excitation (see Figure 8).

first results of the applied Taylor-Hood elements, when we solve the extended conservation equations including convection due to some fluid flow within the propagation region.

References

- [1] D. Braess. *Finite Elemente*. Springer, 2007.
- [2] M. Fortin. Finite element solution of navier-stokes equations. *Acta Numerica*, pages 3239–284, 1993.
- [3] T. Hughes. *The Finite Element Method*. Prentice-Hall, New Jersey, 1 edition, 1987.
- [4] C.-D. Munz, M. Dumbser, and S. Roller. Linearized acoustic perturbation equations for low mach number flow with variable density and temperature mach. *Journal of Computational Physics*, 224:352–364, 2009.
- [5] J. Seo and Y. Moon. Linearized perturbed compressible equations for low mach number aeroacoustics. *Journal of Computational Physics*, 218(702-719), 2006.